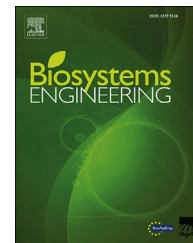




ELSEVIER

Available online at [www.sciencedirect.com](http://www.sciencedirect.com)

ScienceDirect

journal homepage: [www.elsevier.com/locate/issn/15375110](http://www.elsevier.com/locate/issn/15375110)

## Research Paper

# Modeling thin layer drying-roasting kinetics of soaked quinoa. Coupled mass and energy transfer

Ricardo M. Torrez Irigoyen<sup>a,b,\*</sup>, Sergio A. Giner<sup>a,b,c</sup><sup>a</sup> Centro de Investigación y Desarrollo en Criotecología de Alimentos (CIDCA), Universidad Nacional de La Plata-CONICET-CIC, Calle 47 y 116, 1900, La Plata, Argentina<sup>b</sup> Facultad de Ingeniería, Universidad Nacional de La Plata, Argentina<sup>c</sup> Comisión de Investigaciones Científicas de la Provincia de Buenos Aires, Argentina

## ARTICLE INFO

## Article history:

Received 13 July 2016

Received in revised form

22 February 2017

Accepted 10 March 2017

Published online 30 March 2017

## Keywords:

Quinoa

Drying-roasting

Optimization

Fluidisation

Quinoa has higher protein content (11–16% m/m) and better amino acid profile than most cereals and represents a valuable resource for healthy nutrition. This work studied the kinetics of mass and energy transfer during fluidised thin layer drying-roasting of soaked and washed quinoa, a treatment suitable for preparing a ready-to-eat food. Curves describing moisture content and temperature behaviour with time were obtained for temperatures of 80, 100, 120, and 140 °C and air velocity of 0.8 m s<sup>-1</sup>. A coupled mass and energy model was proposed to describe the curves mathematically. The model consisted of a pair of ordinary differential equations (ODEs): a transient macroscopic energy balance equation for heat transfer and either a short or a long dimensionless time mass transfer equation. The model was used to determine the effective diffusion coefficient proposed as an Arrhenius function of temperature by utilising the whole dataset. The heat transfer coefficient was estimated from a correlation reported earlier with values ranging from 164 to 179 W m<sup>-2</sup> °C<sup>-1</sup>. The activation energy and pre-exponential factor were fitted using a combined method involving a numerical integration of the ODE system followed by a parameter optimisation algorithm. Values obtained were  $E_a = 39.9 \text{ kJ mol}^{-1}$  and,  $D_0 = 2.872 \times 10^{-4} \text{ m}^2 \text{ s}^{-1}$ , respectively. Predicted moisture content and temperatures agreed well with experimental values. The present research could be extended to deep fluidised bed models to help optimise existing equipment or design new.

© 2017 IAGrE. Published by Elsevier Ltd. All rights reserved.

## 1. Introduction

Quinoa (*Chenopodium quinoa Willd*) has been cultivated in the Andean regions of Peru, Bolivia and Argentina since the times of the Incas. In Argentina, quinoa is produced in small areas of the Jujuy and Salta provinces (Reinaudi, Grégoire, & Szlápelis,

2002). The protein (11–16% m/m) and minerals content of quinoa are higher than in cereals. It possesses all essential amino acids and its lipid content (5–6% m/m) is mostly composed of essential fatty acids. Having no gluten, quinoa is a food of choice for celiacs (Ridout, Price, DuPont, Parker, Fenwick, 1991). Quinoa grains have become so important that FAO declared 2013 as the International Year of Quinoa

\* Corresponding author. Centro de Investigación y Desarrollo en Criotecología de Alimentos (CIDCA), Universidad Nacional de La Plata-CONICET-CIC, Calle 47 y 116, 1900, La Plata, Argentina

E-mail address: [ricardo\\_mart2@yahoo.com.ar](mailto:ricardo_mart2@yahoo.com.ar) (R.M. Torrez Irigoyen).

<http://dx.doi.org/10.1016/j.biosystemseng.2017.03.003>

1537-5110/© 2017 IAGrE. Published by Elsevier Ltd. All rights reserved.

**Nomenclature**

$a_v$	grain surface area per unit volume, $\text{m}^2 \text{m}^{-3}$
$B$	constant equal to 6547.1, Eq. (13)
$C$	constant equal to 4.23, Eq. (13)
$C_p$	specific heat of grain, $\text{J kg dry matter}^{-1} \text{ }^\circ\text{C}^{-1}$
$D_{eff}$	effective diffusion coefficient of water, $\text{m}^2 \text{s}^{-1}$
$D_0$	pre-exponential factor in $\text{m}^2 \text{s}^{-1}$
$E_a$	activation energy in $\text{kJ mol}^{-1}$
$h_T$	heat transfer coefficient, $\text{W m}^{-2} \text{ }^\circ\text{C}^{-1}$
$L_g$	heat of desorption of water in the grain, $\text{J kg}^{-1}$
$L_w$	latent heat of water vaporization, $\text{J kg}^{-1}$
$M_w$	molar mass of water, $\text{kg kmol}^{-1}$
$r$	radial position, $\text{m}$
$R$	particle radius, $\text{m}$
$R_g$	universal gas constant, $8.314 \times 10^{-3} \text{ kJ mol}^{-1} \text{ K}^{-1}$
$s$	standard deviation
$t$	time, seconds
$T$	grain temperature, $^\circ\text{C}$
$W$	moisture content, $\text{kg water kg dry matter}^{-1}$
$X^2$	dimensionless time defined as $a_v^2 D_{eff} t$

**Subscripts**

$a$	air
$ad$	dimensionless
$e$	equilibrium
$exp$	experimental
$l$	local
$m$	mean
$pred$	predicted
$0$	initial

**Greek symbols**

$\rho_{so}$	dry matter density, $\text{kg m}^{-3}$
$\pi$	constant

(FAO, 2013). However, these grains have bitter antinutrients, the saponins, which are considered toxic in humans, affecting protein digestion (Francis, Kerem, Makkar, & Becker, 2002) hence they must be removed before consumption. Saponin removal (so-called “quinoa washing”) is a solid–liquid extraction process usually carried out domestically by stirring the grains by hand in a strainer under running water. Saponins are assumed to be present when foam occurs during washing. As the foam disappears, the washing is considered complete (Ridout et al., 1991). A method for producing a ready-to-eat grain snack consists of a first stage of soaking the grain to achieve volume expansion, followed by a second stage of rapid drying-roasting in which the grains are cooked at high air temperatures while being simultaneously being stabilised. To achieve a final expansion, the increase of grain volume during soaking should be greater than the shrinkage that occurs during drying-roasting. Using this method grains become lighter, more porous, and have improved consumer acceptability (Torrez Irigoyen and Giner, 2011).

Several mathematical models have been employed to describe drying kinetics; including semi-theoretical and

empirical thin-layer models (Akpınar, 2006; Da Silva, Cleide, Fernando, & Josivanda, 2014; Mohapatra & Rao, 2005; Perea-Flores et al., 2012; Ruhanian & Movagharnjad, 2016; Tanaka, Tanaka, Tanaka, & Toshitaka, 2015). These models are not based on any underlying drying mechanism and their parameters, have no physical meaning. Thus, although these equations may be useful to describe accurately the drying curve for the conditions tested, they are unable to improve the understanding of the processes that occur during drying. Sun and Woods (1994), Gely and Santalla (2007), Da Silva, Precker, Silva, and Silva (2009), Doymaz and İsmail (2011) and Torrez Irigoyen and Giner (2014) have used a different approach resorting to analytical solutions based on a well-founded theory as diffusion to fit the drying curves assuming isothermal conditions. However, this approach requires the diffusion coefficients to be correlated with air temperature, and to ignore the transient nature of the product temperature curve.

Di Scala and Crapiste (2008) used the simplified long time version of the diffusion analytical equation and fitted diffusion coefficients for red pepper assuming isothermal drying conditions. They then used these parameters to predict the coupled non-isothermal mass and energy transfer as a function of time to supply thermal and moisture histories to a product quality model. This approach, although more advanced than those described earlier, was still a simplified method as the parameters were not fitted to the simultaneous drying and heating curves. Hertog, Verlinden, Lammertyn, and Nicolai (2007) developed an optimisation extension to MatLab (MathWorks, Inc., Natick, MA, USA) called OptiPa (Katholieke Universiteit Leuven, Belgium) that allows parameters to be optimised during the integration of single or sets of, ordinary differential equations (ODEs). Schouten, Farneti, Tijksens, Alarcón, and Woltering (2014) when quantifying lycopene and chlorophyll in tomato and Amodio, Derossi, and Colelli (2014), when modelling the phenolic content during storage of fruit and vegetables, used this software and obtained accurate predictions. However, this method was not applied so far to the study of drying kinetics.

As an essential step to aid process design for manufacturing a ready-to-eat quinoa grain snack, this work studied the drying-roasting kinetics of quinoa by using an ODE system to represent coupled mass and energy transfer. From the system parameters were optimised using an ODE numerical solver combined with a parameter optimisation procedure (OptiPa).

## 2. Material and methods

### 2.1. Material

Quinoa grains of the CICA cultivar, provided by the INTA EEA Famaillá, Provincia de Tucumán, Argentina (Famaillá Experimental Station of the National Institute of Agricultural Technology, Province of Tucumán) were utilised. Moisture content at reception was  $0.111 \text{ kg [water] kg}^{-1} \text{ [dry matter]}$ . The experimental work carried out can be described by the flow sheet shown in Fig. 1.

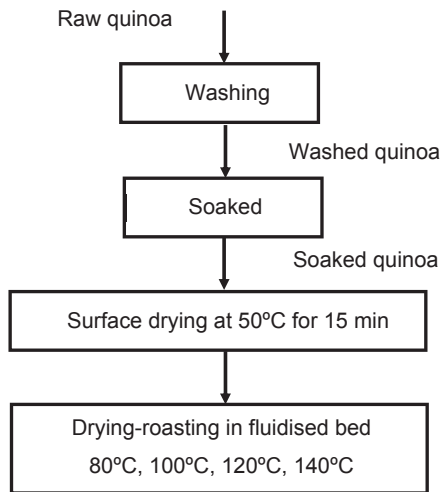


Fig. 1 – Experimental plan followed in this work.

### 2.2. Determination of moisture content

Moisture content was determined in triplicate by the AOCs Ac 2-41 method (130 °C, atmospheric pressure, 3 h) in a mechanical convection oven (Model SL30SDB, SAN JOR, Buenos Aires, Argentina) using an air velocity of 0.25 m s<sup>-1</sup>.

### 2.3. Determination of quinoa volume and radius

The volume ( $V_0$ ) of soaked quinoa grains was determined by a pycnometric method described in [Torrez Irigoyen and Giner \(2011\)](#). The value was averaged over 10 replicates and, from it, the equivalent spherical diameter ( $D_e$ ) was calculated.

### 2.4. Soaking and washing for saponin removal

Grains were visually inspected to remove foreign materials and then immersed in drinking water, using a 3:1 water to quinoa mass ratio, and allowed to soak for 15 min at 20 °C. Then, the samples were washed for 30 min in running water until no foam formation was observed ([Ridout et al., 1991](#)).

### 2.5. Surface drying

In order to improve the fluidisation properties of soaked-washed quinoa for drying-roasting, grains were surface-dried in the mechanical convection oven mentioned above set at 50 °C for 15 min. For all cases the average initial moisture content after soaking and surface drying, was 0.820 kg [water] kg<sup>-1</sup> [dry matter].

### 2.6. Fluidised bed equipment

Figure 2 shows a drawing of the bench scale dryer used to conduct the kinetic experiments. This was designed to process fluidised beds up to 0.2 m deep, though in this work it was utilised to study drying kinetics in a fluidised thin layer. There are six main parts in the equipment: A) a thermally insulated drying chamber, 0.10 m internal diameter and 0.3 m in height with a double glazing inspection window made of borosilicate

glass, B) a Testo 525 micromanometer with range 0–25 hPa and error ±0.2% at full scale (Testo AG, Lenzkirch Germany) to measure pressure differences through the bed, C) An electronic temperature controller, which include a software developed in Java that allowed the temperature of the air entering the chamber to be set (inlet air temperature), D) a variable-frequency drive to control the air velocity by regulating the angular fan speed (Model CFW-08, WEG, Jaraguá do Sul, Brazil), E) a Testo 435 hot wire anemometer (Testo AG, Lenzkirch Germany) to measure air velocity upstream the chamber in cold airflow through a duct 1 m in length, and F) a centrifugal fan, powered with a 0.55 kW electric motor (maximum rotational speed, 2800 rpm).

### 2.7. Drying-roasting in fluidised thin layer

The moisture content of quinoa was measured as a function of time at air temperatures of 80, 100, 120 and 140 °C, and an air velocity of 0.8 m s<sup>-1</sup>. The equipment was turned on and, once the air temperature became stable, a grain layer 0.01 m deep was loaded to the chamber (average initial mass of grains: 31.01 ± 0.7 g). Samples were removed on several occasions between 0 and 30 min for moisture content analysis. The thin-layer drying nature of the system (i.e, constant air conditions along each experiment) was not altered by this procedure. The thermal history of grains was recorded using a non-contact infrared thermometer Testo 830 T2 ((Testo AG, Lenzkirch Germany)). Each temperature recorded was an average of three readings, carried out every two minutes during the process.

### 2.8. Mathematical modelling of drying-roasting

#### 2.8.1. Analytical solutions of the diffusion equation

Considering the partial differential equation for diffusion in a sphere,

$$\frac{\partial W_1}{\partial t} = D_{eff} \left( \frac{\partial^2 W_1}{\partial r^2} + \frac{2}{r} \frac{\partial W_1}{\partial r} \right) \quad (1)$$

Where  $W_1$  is the local moisture content kg [water] kg [dry matter]<sup>-1</sup>,  $D_{eff}$  effective diffusion coefficient m<sup>2</sup> s<sup>-1</sup> and  $r$  is the radial position in m. The initial and boundary conditions are the following

$$t = 0 \quad W_1 = W_0 \quad 0 \leq r \leq R \quad (2)$$

$$r = 0 \quad \frac{\partial W_1}{\partial r} = 0 \quad t > 0 \quad (3)$$

$$r = R \quad W = W_e \quad t > 0 \quad (4)$$

where  $W_0$  is the initial moisture content kg [water] kg [dry matter]<sup>-1</sup> and  $R$  the grain radius in m. An analytical series solution has been obtained by integrating the diffusion equation for the whole grain ([Doymaz & İsmail, 2011](#)).

$$W_{ad} = \frac{W_m - W_e}{W_0 - W_e} = \frac{6}{\pi^2} \sum_{n=1}^{n=\infty} \frac{1}{n^2} \exp \left[ -n^2 \pi^2 \left( \frac{D_{eff} t}{R^2} \right) \right] \quad (5)$$

where  $W_{ad}$  is the dimensionless moisture content,  $W_m$  the mean quinoa moisture content at time  $t$  in s,  $W_e$  the

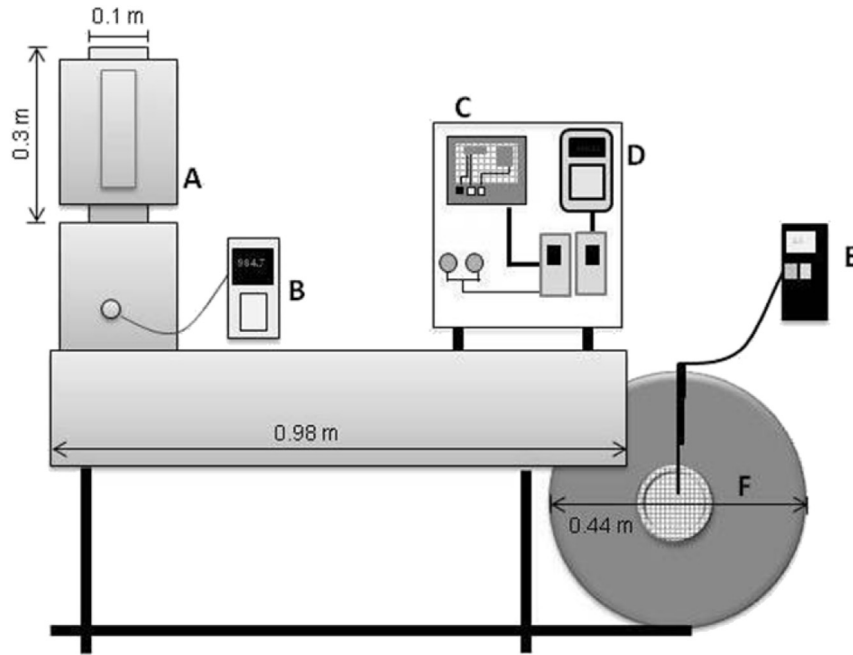


**Fig. 2 – (A) Drying chamber, (B) Digital micromanometer, (C) Electronic circuit temperature controller, (D) Fan speed controller, (E) Digital hot-wire anemometer, (F) Centrifugal fan.**

equilibrium moisture content in  $\text{kg} [\text{water}] \text{kg} [\text{dry matter}]^{-1}$  and  $n$  a positive integer. This equation describes the variation of the mean grain moisture content with time.

The strict internal control to the mass transfer rate usually observed in grains is reinforced by the high air velocities used in fluidisation, that reduce the thickness of the external boundary layer surrounding the grain to a minimum and makes its resistance to mass transfer negligible compared with the diffusional contribution of the grain itself. The initial radius of soaked quinoa had an average value of  $1.58 \times 10^{-3}$  m. The equilibrium moisture content of grains ( $W_e$ ) for each temperature was pre-estimated using the modified GAB equation for quinoa (Torreba, Peltzer, Enriquez, & Pollio, 2004). However, as the values computed were close to zero the value of  $W_e$  was taken as 0 in all experiments.

Torrez Irigoyen and Giner (2014) observed that using the analytical solution for spheres and with constant  $D_{eff}$  and constant  $R$ , during the drying–toasting of soaked soybean yielded accurate predictions. This was despite a non-negligible shrinkage occurring during thermal process which had been observed earlier (Torrez Irigoyen and Giner, 2011). This unexpectedly accurate prediction for soybean was thought to be caused by the substantially constant ratio of  $D_{eff}$  to  $R^2$  found in Eq. (5).

There is an alternative analytical solution of the diffusion equation (Becker, 1959) which is based on the concept of a semi-infinite medium, valid for short dimensionless times  $X^2 < 1$  ( $X^2 = a_v^2 D_{eff} t$  where  $a_v$  is the grain surface area per unit volume, yielding  $3/R$  for spherical geometry) or dimensionless mean moisture contents in the range  $0.2 < W_{ad} < 1$ , where the approximate expression, Eq. (6),

coincides with Eq. (5). For equivalent spheres, the equation is

$$W_{ad} = \frac{W_m - W_e}{W_0 - W_e} = 1 - \frac{2}{\sqrt{\pi}} \left( \frac{3}{R} \right) \sqrt{D_{eff} t} + 0.331 \left( \frac{3}{R} \right)^2 D_{eff} t \quad (6)$$

This short times equation (STE) has been applied successfully to postharvest drying data of raw soybean (Gely & Giner, 2007).

### 2.8.2. Dependence of the diffusion coefficient with temperature

In order to consider  $D_{eff}$  dependence with temperature within the model, an Arrhenius-type equation, was proposed in (Eq. (7)):

$$D_{(T)} = D_0 \exp \left( - \frac{E_a}{R_g (T + 273.15)} \right) \quad (7)$$

where  $D_0$  is the pre-exponential factor in  $\text{m}^2 \text{s}^{-1}$ ,  $E_a$  the activation energy in  $\text{kJ mol}^{-1}$  and  $R_g$  the universal gas constant,  $8.314 \times 10^{-3} \text{ kJ mol}^{-1} \text{ K}^{-1}$ , being  $T$  is the grain temperature  $^{\circ}\text{C}$ .

### 2.8.3. Macroscopic energy balance

Grain temperature was assumed to be uniform, i.e. the internal temperature profile in the grain is flat, though variable with time (Rodríguez-Fernández, Balsa-Canto, Egea, & Banga, 2007). This is because the heat transfer Biot number for drying tends to zero in small particles (Torrez Irigoyen et al., 2014). A more detailed analysis based on the Biot number for heat and mass transfer during drying was given by Giner, Torreba Irigoyen, Cicuttin, and Fiorentini (2010). Heat transfer between air and grain is a phenomenon governed by external

control. Thus, the macroscopic energy balance for the thin layer of grains can be represented by the following expression:

$$\rho_{so} C_p \frac{dT}{dt} = h_T a_v (T_a - T) - \rho_{so} \left( \frac{dW_m}{dt} \right) L_w \quad (8)$$

where  $dT/dt$  is the heating rate and  $(-dW_m/dt)$  the drying rate based on the mean moisture content. The symbol  $\rho_{so}$  is the dry matter density,  $\text{kg m}^{-3}$ ,  $C_p$  the specific heat of grain,  $\text{J kg [dry matter]}^{-1} \text{ }^\circ\text{C}^{-1}$ ,  $h_T$  is the heat transfer coefficient,  $\text{W m}^{-2} \text{ }^\circ\text{C}^{-1}$ ,  $L_w$  the latent heat of water vaporization,  $\text{J kg}^{-1}$  and  $T_a$  the air temperature in  $^\circ\text{C}$ .

Equation (8) represents an ordinary differential equation with variable coefficients which have the initial condition  $t = t_0$  at  $T = T_0$ . The derivatives are total because, as indicated before, the temperature profile is assumed to be flat, whereas  $W_m$  is a spatially integrated average value inside the sphere (Giner et al., 2010). The specific heat and heat of desorption were evaluated using the average moisture content and grain temperature, respectively (Torrez Irigoyen et al., 2014). A similar model for heat transfer was used by Simal, Mulet, Catala, Cañelas, and Rosselló (1996) and Rahman and Kumar (2006), who studied the drying of foods. In this work, the gas-particle heat transfer coefficient ( $h_T$ ) was calculated by the correlation developed by Vazquez and Calvelo (1983) for fluidization of different shaped foods.

#### 2.8.4. Coupled mass and energy transfer

To develop a kinetic model adapted to parameter fitting under the non-isothermal conditions that prevail during drying-roasting, a system of ordinary differential equations (ODE) was developed. This enabled us to fit the activation energy ( $E_a$ ) and pre-exponential factor ( $D_0$ ) to all the datasets of moisture contents and temperatures as a function of time. With this purpose in mind Eqs. (5) and (8) were derived with respect to time, so that the following ODEs were obtained:

$$\frac{dW_m}{dt} = -(W_0 - W_e) \frac{6}{R^2} \left( D_0 \exp\left(-\frac{E_a}{R_g(T + 273.15)}\right) \right) \times \sum_{n=1}^{n=\infty} \exp\left[-\frac{1}{n^2} \pi^2 \left( D_0 \exp\left(-\frac{E_a}{R_g(T + 273.15)}\right) \frac{t}{R^2} \right)\right] \quad (9)$$

$$\frac{dT}{dt} = \frac{h_T \left(\frac{a}{R}\right) (T_a - T)}{\rho_{so} C_p} - \left(-\frac{dW_m}{dt}\right) \frac{L_w}{C_p} \quad (10)$$

The calculation sequence is as follows: given the initial values ( $t = t_0$ ,  $W = W_0$ ,  $T = T_0$ ), and initial estimates for  $D_0$  and  $E_a$ , calculations were started at  $t = t_0$  by computing the drying rate ( $dW_m/dt$ ) from Eq. (9); then this drying rate was utilised in the heat transfer equation (10) to compute  $dT/dt$ . Both ODEs were integrated to the following time value,  $t + \Delta t$  and this sequence was repeated over the duration of the experiment being simulated.

The following relationships were also used in the ODE system:

**Specific heat**, in  $\text{J kg}^{-1}$  [dry matter]  $^\circ\text{C}^{-1}$  was computed by expressions given by Mohsenin (1980) and previously utilised by Torrez Irigoyen et al. (2014).

For moisture contents  $< 0.7$  kg [water]  $\text{kg}^{-1}$  [dry matter]:

$$C_p = 1638.08 + 3566.19 W_m \quad (11)$$

For moisture contents  $\geq 0.7$  kg [water]  $\text{kg}^{-1}$  [dry matter]

$$C_p = 837.4 + 4187 W_m \quad (12)$$

**Heat transfer coefficient** was estimated using correlations developed by Vazquez and Calvelo (1980) for the fluidised bed treatment of peas and aluminium spheres. The values obtained were: 179.20; 173.80; 168.82 and 164.22 in  $\text{W m}^{-2} \text{ }^\circ\text{C}^{-1}$  for 80, 100, 120 and 140  $^\circ\text{C}$  respectively. These values are within the range given by Souraki, André, and Mowla (2009) of 100–400  $\text{W m}^{-2} \text{ }^\circ\text{C}^{-1}$  for fluidised bed treatments and Vazquez and Calvelo (1983) for the fluidisation of differently shaped foods. These authors considered that the high values of  $h_T$  found here are due to the high degree of mixing experienced by particles inside the drying chamber.

**Heat of desorption of water in grain ( $L_g$ )** was based on the results obtained by Torrez Irigoyen and Giner (2014) who did not observe an effect of temperature on water activity in soaked and partially dried-toasted soybeans ( $L_w = L_g$ ) was calculated from the Clapeyron equation for the latent heat of pure water vaporisation, i.e., only temperature dependent:

$$L_w = \frac{R_g}{M_w} (B - C(T + 273.16)) \quad (13)$$

where  $M_w$  is the molar mass of water,  $\text{kg kmol}^{-1}$ , and  $B = 6547.1$  and  $C = 4.23$  from the Kiefer's saturation vapour pressure correlation (Giner, 2001).

#### 2.8.5. Fitting procedure: integration of the ODE followed by parameter optimization

Parameters to be fitted from the differential equations, and especially those depending on the system unknowns (temperature or moisture content), constitute a nonlinear inverse problem which cannot be dealt with the conventional statistical packages designed for integral equations. In this work, both the integration of the ODE system and the corresponding parameter optimisation steps were carried out using the OptiPa software (Hertog et al., 2007) with initial values of  $E_a$  and  $D_0$  obtained by fitting integral analytical solutions to drying-toasting curves from pre-soaked soybean assuming an isothermal process (Torrez Irigoyen and Giner, 2014).

Due to the stiff nature of the differential equations, once the predicted moisture and temperature curves were calculated using the Matlab ode23solver selected among various options in OptiPa software, the predicted curves were compared to the measured data and the sum of the residuals squared was used to feed the parameter optimisation algorithm to provide a better estimate of the unknown parameters. This integration-optimisation cycle was repeated until the sum of the residuals squared was minimised. The specific least squares non-linear optimisation routine used was the Levenberg–Marquardt method which is available in the OptiPa software package. The residuals squared of both moisture contents and temperatures were normalised by using the standard deviation squared of the set of experimental data. Such residuals squared were summed over all the experiments involved (in this case four runs each measured in triplicate) as indicated in Eq. (14). Normalising the residuals squared allows the system to work on a dimensionless basis and therefore it was possible to sum residuals of different dependent variables to reach a combined least squares optimisation criterion.

$$SSR = \frac{1}{S_{W_{exp}}^2} \sum_{j=1}^k (W_{mj} - W_{exp,j})^2 + \frac{1}{S_{T_{exp}}^2} \sum_{j=1}^k (T_j - T_{exp,j})^2 \quad (14)$$

where  $s$  is the standard deviation, and the subscript  $exp$  represents the experimental values.

### 2.9. Statistical analysis

Triplicate experiments were carried out for each drying-roasting condition, measuring moisture content and temperature. Different experimental conditions were compared by the Tukey's test (Montgomery, 1991), at a confidence level of 95%. For each dependent variable, the goodness of fit was evaluated by two indicators. The indicator expressed in the same units as the fitted variable is the root mean square error (RMSE)

$$RMSE = \sqrt{\frac{\sum_{i=1}^p (y_{pred,i} - y_{exp,i})^2}{p}} \quad (15)$$

where  $y_{exp,i}$  is an experimental value and  $y_{pred,i}$  represents the corresponding predicted number. The other statistical indicator is the coefficient of determination  $r^2$ , which was computed as well for each dependent variable by using the following equation

$$r^2 = 1 - \frac{\sum_{i=1}^p (y_{exp,i} - y_{pred,i})^2}{\sum_{i=1}^p (y_{exp,i} - y_m)^2} \quad (16)$$

where  $y_m$  is the arithmetic average of the experimental values.

## 3. Results and discussion

### 3.1. Experimental drying curves

The Tukey's test revealed non-significant differences (at a confidence level of 95%) among triplicates of moisture content and temperatures in all experiments. The observed drying

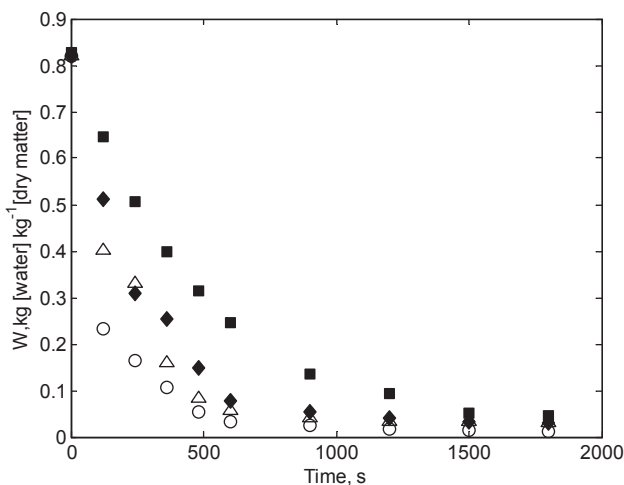


**Fig. 3 – Experimental curves of quinoa moisture content as a function of time, at various air temperatures: (■) 80 °C, (◆) 100 °C, (△) 120 °C and (○) 140 °C.**

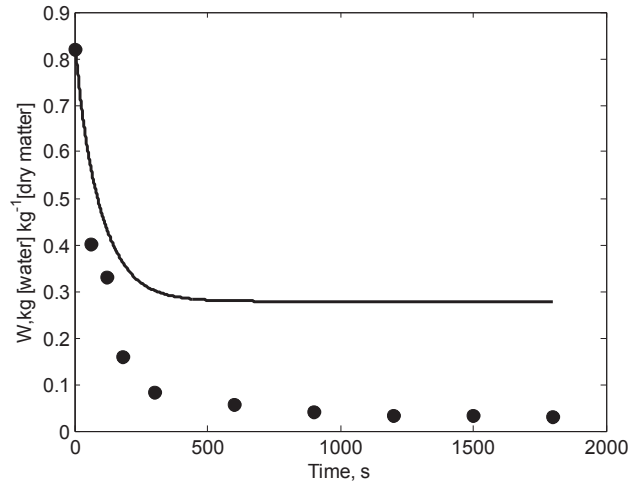


**Fig. 4 – Thin-layer drying-roasting of soaked quinoa. Experimental data (symbols), and predicted values (—) solving coupled mass and energy model (Eq. (9)), for inlet air temperature of 120 °C.**

roasting curves represent the mean moisture content ( $W_m$ ) as a function of time, in  $\text{kg [water] kg}^{-1} [\text{dry matter}]$ .

As observed from Fig. 3, the drying-roasting curves showed a sharp decrease in moisture content with time and the slope, represented by the drying rate, decreased in absolute terms with the progress of drying. This denotes a strong internal control for mass transfer as well as a gradual approach towards equilibrium with the air. In addition, the moisture content drop is faster at higher temperatures and this aspect posed a difficulty for measuring the data, as samples had to be removed at shorter time intervals, particularly at the beginning of the drying-roasting of this small grain. Gely and Santalla (2007) have reported a similar behaviour on postharvest drying of raw quinoa in a lower temperature range (30–90 °C), as did Perea-Flores et al. (2012) when studying the drying of castor beans between 80 and 110 °C.

### 3.2. Modelling coupled energy and mass transfer

The coupled mass and transfer model represented by Eqs. (9)–(13) was fitted to data by the integration-optimisation procedure described in Section 2.8.5. However, prediction of moisture content was inadequate in all treatments. For

**Table 1 – Fitting the coupled mass and energy transfer model during drying-roasting of soaked quinoa used to estimate the activation energy and pre-exponential factor. RMSE (with units of the dependent variable) and  $r^2$  for the whole dataset.**

Variable	$r^2$	RMSE
W	0.981	0.035
T	0.999	1.126

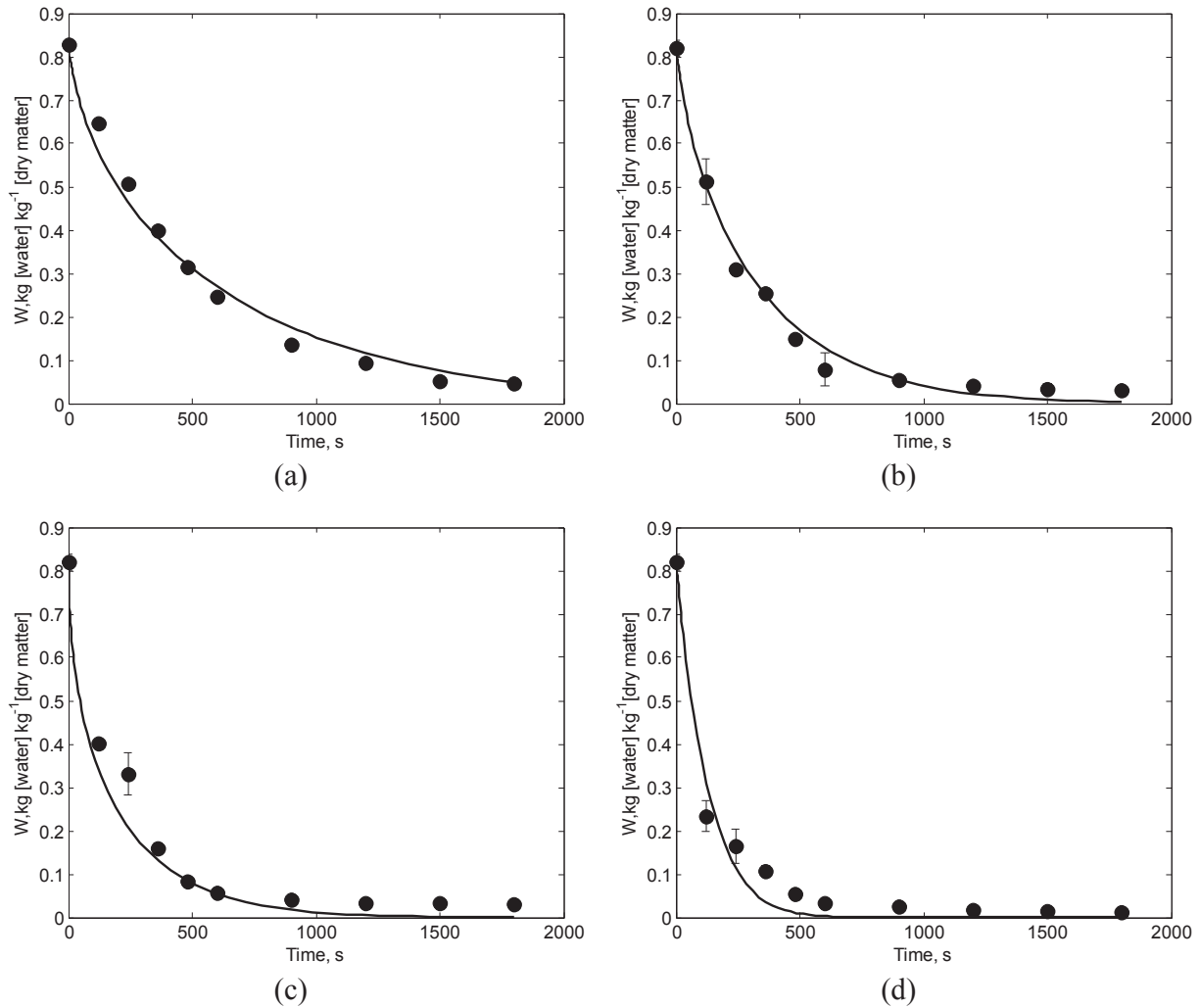


**Fig. 5 – Thin-layer drying-roasting of soaked quinoa. Experimental data (symbols), and curves (lines) predicted by solving the coupled mass and energy model with the optimised parameters, for air temperatures of: (a) 80 °C, (b) 100 °C, (c) 120 °C and (d) 140 °C.**

instance, Fig. 4 shows the results of moisture content vs time obtained for an air temperature of 120 °C.

As these predictions were surprisingly poor, an expert in the field of ordinary differential equations applied to foods was consulted (Dr. Marteen Hertog, 2016, personal communication). His advice was not to use derivatives with exponential terms, which would tend to zero when calculated in a computer program. The cause is the truncation of very small values in limited memory allocation of numbers, particularly when time is long. A better method was to replace them by equivalent expressions based on the driving force. Giner (2001) found a similar behaviour for long times during the modelling of the postharvest drying of wheat in fixed beds.

The results mentioned earlier led us to propose an original procedure by which the fitting equation for the mass transfer rate in the ODE system was alternatively the derivative with time of the diffusion equation for short ( $X^2 < 1$ )

or long dimensionless times ( $X^2 > 1$ ), the latter being represented by one term of Eq. (9). The exponential factor in the derivative of the long time equation was replaced by a mathematically (though not numerically) equivalent expression (Eq. (17)).

For  $X^2 \leq 1$

$$W_m = W_e + (W_0 - W_e) \left[ 1 - \frac{2}{\sqrt{\pi}} \left( \frac{3}{R} \right) \sqrt{D_{eff} t} + 0,331 \left( \frac{3}{R} \right)^2 D_{eff} t \right] \quad (17)$$

$$\frac{dW_m}{dt} = -(W_0 - W_e) \left[ \left( \frac{3}{R} \right) \sqrt{\frac{D_{eff}}{\pi t}} - 0,331 \left( \frac{3}{R} \right)^2 D_{eff} \right] \quad (18)$$

Then, replacing the invariant driving force ( $W_0 - W_e$ ) by a variable one ( $W_m - W_e$ ) based on Eq. (17) and expressing the symbol  $D_{eff}$  by the Arrhenius relationship Eq. (7), we have

$$\frac{dW_m}{dt} = -(W_m - W_e) \frac{\left[ \left(\frac{3}{R}\right) \sqrt{\frac{D_0 \exp\left(-\frac{E_a}{R_g(T+273.15)}\right)}{\pi t}} - 0.331 \left(\frac{3}{R}\right)^2 \left(D_0 \exp\left(-\frac{E_a}{R_g(T+273.15)}\right)\right) \right]}{\left[ 1 - \frac{2}{\sqrt{\pi}} \left(\frac{3}{R}\right) \sqrt{\left(D_0 \exp\left(-\frac{E_a}{R_g(T+273.15)}\right)\right) t} + 0.331 \left(\frac{3}{R}\right)^2 \left(D_0 \exp\left(-\frac{E_a}{R_g(T+273.15)}\right)\right) t \right]} \quad (19)$$

For  $X^2 > 1$

$$W_m = W_e + (W_0 - W_e) \frac{6}{\pi^2} \exp\left[-\frac{\pi^2}{9} \left(\frac{3}{R}\right)^2 D_{eff} t\right] \quad (20)$$

$$\frac{dW_m}{dt} = -\left[-\frac{\pi^2}{9} \left(\frac{3}{R}\right)^2 D_{eff}\right] (W_0 - W_e) \frac{6}{\pi^2} \exp\left[-\frac{\pi^2}{9} \left(\frac{3}{R}\right)^2 D_{eff} t\right] \quad (21)$$

In order to express Eq. (21) by an equivalent equation based on a variable driving force and replacing  $D_{eff}$  as earlier, we find

$$\frac{dW_m}{dt} = -(W_m - W_e) \left[ \pi^2 \frac{\left(\frac{3}{R}\right)^2}{9} \left(D_0 \exp\left(-\frac{E_a}{R_g(T+273.15)}\right)\right) \right] \quad (22)$$

This procedure is innovative, because no drying kinetics studies using two alternative fitting equations for mass transfer could be found in the literature and even less under non-isothermal conditions. An earlier work by Giner (2001) applied two alternative equations for simulation purposes but not for fitting mass transfer parameters. This is a new aspect within the already novel

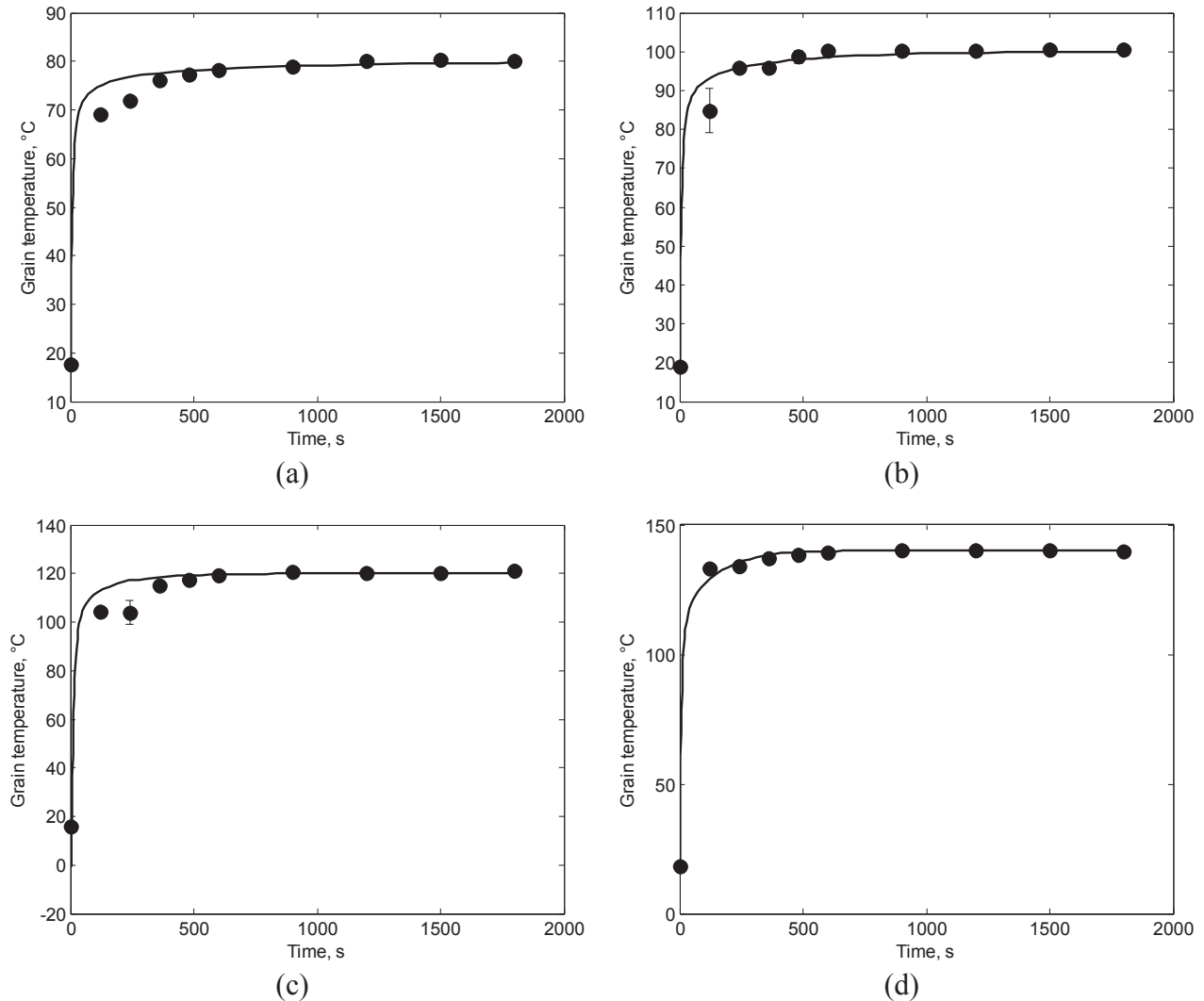


**Fig. 6 – Grain temperature as a function of drying-roasting time. Experimental values (symbols) and curves (solid lines) predicted by solving the coupled mass and energy transfer model with the optimized parameters in various air conditions: (a) 80 °C, (b) 100 °C, (c) 120 °C and (d) 140 °C.**



procedure of fitting parameters based on an ODE system for drying.

### 3.3. Fitting mass transfer parameters from the coupled mass and energy transfer model

Table 1 shows the results of fitting the drying-roasting model, Eqs. (19) and (22), to the experimental curves of moisture content and temperature as a function of time. An accurate agreement was achieved, with an activation energy  $E_a = 39.9$  (1.14) kJ mol<sup>-1</sup> and pre-exponential factor of  $2.872 \times 10^{-4}$  ( $1.109 \times 10^{-4}$ ) m<sup>2</sup> s<sup>-1</sup>. The coefficient of determination was of 0.998 for the two variables considered together. The values presented in parenthesis are the standard deviation of the parameters. The parameters determined from the ODE system were better founded and have more physical meaning because the whole dataset was considered to solve a non-isothermal, coupled mass and energy transfer model. Values of the activation energy were consistent with a previous study (Fiorentini, Demarchi, Quintero Ruiz, Torrez Irigoyen, & Giner, 2015) and within the values published by other authors who worked under conditions of low moisture content and moderate drying temperatures. For instance, Gely and Santalla (2007) in the postharvest drying of quinoa seeds obtained 37.9 kJ mol<sup>-1</sup> and Doymaz (2005), studying bean drying found  $E_a = 35.4$  kJ mol<sup>-1</sup>. In a recent work, Torrez Irigoyen and Giner (2014) found an activation energy around 31.4 kJ mol<sup>-1</sup> in the drying-toasting of soaked soybeans. All previous values were determined by fitting integral equations that assumed isothermal conditions, unlike in this work where the fitting was carried out with a non-isothermal model.

Figure 5 shows experimental moisture content as a function of time, for all drying-roasting treatments as well as the predicted curves. For all air temperatures, a good agreement was observed. Thus, the combination of the diffusion equations for short and long dimensionless times yielded accurate predictions. The validity of each equation is subject to the limits imposed by the dimensionless time.

Figure 6 shows the variation of the grain temperature with drying-roasting time and the predicted values. As can be seen for all treatments, a satisfactory agreement was obtained. Increasing air temperatures led to higher heating rates, and all curves tended to their corresponding air temperature asymptotes after about 500 s. This fast approach to the limiting temperature is a consequence of the small particle size of quinoa. Torrez Irigoyen et al. (2014) who studied the drying-toasting of pre-cooked soybeans found a slower heating rate related with the larger sized soaked soybeans.

Thus, the results obtained for temperature and moisture content curves demonstrate that the model developed was able to fit the parameters considering the simultaneous mass and energy transfer phenomena involved in the thermal treatment.

## 4. Conclusions

To provide information for the production of an innovative snack using a fluidisation technique, data was obtained on the

drying-roasting of washed quinoa at temperatures from 80 to 140 °C and a mathematical model developed.

A coupled mass and energy balance problem was represented by a system of two ordinary differential equations (ODE), using the derivative of an analytical solution of the diffusion equation in the form of an infinite series for predicting the drying rate and a transient macroscopic energy balance for heat transfer. The results showed that this drying rate equation was not suitable because its exponential terms used developed increasingly negative arguments as a function of time which led to a computational artefact that predicted a drying rate close to zero well before this being observed experimentally.

Therefore, the ODE system was reformulated as being the drying rate calculated either by (1), a simplified diffusion equation, valid for short dimensionless times (STE), or (2) the series solution, which, at longer times converges with one term. This allows the exponential term to be replaced by a mathematically equivalent expression which is not an explicit function of time, thus eliminating the computational artefact. The effective diffusion coefficient was evaluated as a function of grain temperature in the Arrhenius type equation. An activation energy ( $E_a$ ) of 39.9 kJ mol<sup>-1</sup> and a pre-exponential factor equal to  $2.872 \times 10^{-4}$  m<sup>2</sup> s<sup>-1</sup> were estimated with an optimisation procedure in the OptiPa software and utilising the whole dataset. Unlike the isothermal method, which only considers the range of drying air temperatures, the non-isothermal method allows the Arrhenius equation to be valid in the whole range of the transient temperature curve, i.e., from the initial product value to reaching drying air temperature. Both predicted moisture and temperature curves were in good agreement with the experimental measurements. The use of temperature variations while fitting parameters permits a more realistic determination of the effective diffusion coefficient and a physically better founded value of the activation energy.

In future work, the model developed here will be extended to a fluidised bed, considering both variations in air temperature and humidity throughout the bed. The results obtained will be useful for technical purposes in process design. In this regard, an accurate activation energy will be critical for calculations of product quality as well as for dryer energy consumption as a function of temperature.

## Acknowledgements

The authors wish to express their gratitude to PhD Maarten Hertog, at Katholieke Universiteit Leuven, Belgium, for his expert and generous advice in general and with programming the OptiPa software in particular.

## REFERENCES

- Akpınar, E. K. (2006). Determination of suitable thin layer drying curve model for some vegetables and fruits. *Journal of Food engineering*, 73, 75–84.
- Amodio, M. L., Derossi, A., & Colelli, G. (2014). Modeling phenolic content during storage of cut fruit and vegetable: A

- consecutive reaction mechanism. *Journal of Food Engineering*, 140, 1–8.
- Becker, H. A. (1959). A study of diffusion in solids of arbitrary shape with application to the drying of the wheat kernel. *Journal Applied Polymer Science*, 1(2), 212–226.
- Da Silva, W. P., Cleide, M. D. P. S., Fernando, J. A., & Josivanda, P. G. (2014). Mathematical models to describe thin-layer drying and to determine drying rate of whole bananas. *Journal of the Saudi Society of Agricultural Sciences*, 13, 67–74.
- Da Silva, W. P., Precker, J. W., Silva, C. M. D. P. S., & Silva, D. D. P. S. (2009). Determination of the effective diffusivity via minimization of the objective function by scanning: Application to drying of cowpea. *Journal of Food Engineering*, 95, 298–304.
- Di Scala, K., & Crapiste, G. (2008). Drying kinetics and quality changes during drying of red pepper. *Lebensmittel Wissenschaft und Technologie*, 41, 789–795.
- Doymaz, I. (2005). Drying behaviour of green beans. *Journal of Food Engineering*, 69, 161–165.
- Doymaz, I., & İsmail, O. (2011). Drying characteristics of sweet cherry. *Food and Bioproducts Processing*, 89, 31–38.
- FAO. (2013). *Food and agriculture organization of the United Nations*. <http://www.fao.org/quinoa-2013/en/>.
- Fiorentini, C., Demarchi, S. M., Quintero Ruiz, N. A., Torrez Irigoyen, R. M., & Giner, S. A. (2015). Arrhenius activation energy for water diffusion during drying of tomato leathers: The concept of characteristic product temperature. *Biosystems Engineering*, 132, 39–46.
- Francis, G., Kerem, Z., Makkar, H. P. S., & Becker, K. (2002). The biological action of saponins in animal systems: A review. *British Journal of Nutrition*, 88, 587–605.
- Gely, M. C., & Giner, S. A. (2007). Diffusion coefficient relationships during drying of soya bean cultivars. *Biosystems Engineering*, 96(2), 213–222.
- Gely, M. C., & Santalla, E. M. (2007). Moisture diffusivity in quinoa (*Chenopodium quinoa willd.*) seeds: Effect of air temperature and initial moisture content of seeds. *Journal of Food Engineering*, 78, 1029–1033.
- Giner, S. A. (2001). An improve cross-flow wheat drying model for equipment design. *Acta Horticae*, 566, 467–476.
- Giner, S. A., Torrez Irigoyen, R. M., Cicuttin, S., & Fiorentini, C. (2010). The variable nature of biot numbers in food drying. *Journal of Food Engineering*, 101, 214–222.
- Hertog, M. L. A. T. (2016). *Personal communication*, BIOSYST-MeBioS. Belgium: Katholieke Universiteit Leuven.
- Hertog, M. L. A. T., Verlinden, B. E., Lammertyn, J., & Nicolai, B. M. (2007). OptiPa, an essential primer to develop models in the postharvest area. *Computers and Electronics in Agriculture*, 57, 99–106.
- Mohapatra, D., & Rao, P. S. (2005). A thin layer drying model of parboiled wheat. *Journal of Food Engineering*, 66, 513–518.
- Mohsenin, N. N. (1980). *Thermal properties of food and agricultural materials*. New York: Gordon and Breach Science Publishers.
- Montgomery, D. C. (1991). *Design and analysis of experiments* (3rd ed.). New York: USA. John Wiley & Sons Inc.,
- Perea-Flores, M. J., Garibay-Flebes, V., Chanona-Pérez, J. J., Calderón-Domínguez, G., Méndez-Méndez, J. V., Palacios-González, E., et al. (2012). Mathematical modelling of castor oil seeds (*Ricinus communis*) drying kinetics in fluidized bed at high temperatures. *Industrial Crops and Products*, 38, 64–71.
- Rahman, N., & Kumar, S. (2006). Evaluation of convective heat transfer coefficient during drying of shrinking bodies. *Energy Conversion and Management*, 47, 2591–2601.
- Reinaudi, N. B., Grégoire, H. C., & Szlápelis, S. E. (2002). *Cultivo de la quinoa Chenopodium quinoa Willd, variedad Blanca de Junín en la región pampeana. Encuentro Bromatológico Latinoamericano*. Córdoba, Argentina: Universidad Católica Argentina, 26 y 27 de Septiembre.
- Ridout, C. L., Price, K. R., DuPont, M. S., Parker, M. L., & Fenwick, G. R. (1991). Quinoa saponins - Analysis and preliminary investigations into the effects of reduction by processing. *Journal of the Science of Food and Agriculture*, 54, 165–176.
- Rodríguez-Fernández, M., Balsa-Canto, E., Egea, J. A., & Banga, J. R. (2007). Identifiability and robust parameter estimation in food process modeling: Application to a drying model. *Journal of Food Engineering*, 83(3), 374–383.
- Ruhanian, S., & Movagharejad, K. (2016). Mathematical modeling and experimental analysis of potato thin-layer drying in an infrared-convective dryer. *Engineering in Agriculture, Environment and Food*, 9, 84–91.
- Schouten, R. E., Farneti, B., Tijsskens, L. M. M., Alarcón, A. A., & Woltering, E. J. (2014). Quantifying lycopene synthesis and chlorophyll breakdown in tomato fruit using remittance VIS spectroscopy. *Postharvest Biology and Technology*, 96, 53–63.
- Simal, S., Mulet, A., Catala, P. J., Cañelas, J., & Rosselló, C. (1996). Moving boundary model for simulating moisture movement in grapes. *Journal of Food Science*, 61(1), 157–160.
- Souraki, B. A., André, A., & Mowla, D. (2009). Mathematical modeling of microwave-assisted inert medium fluidized bed drying of cylindrical carrot samples. *Chemical Engineering and Processing*, 48, 296–305.
- Sun, D., & Woods, J. L. (1994). Low temperature moisture transfer characteristics of barley: Thin-layer models and equilibrium isotherms. *Journal Agricultural Engineering Research*, 59, 273–283.
- Tanaka, F., Tanaka, F., Tanaka, A., & Toshitaka, U. (2015). Mathematical modeling of thin-layer drying according to particle size distribution in crushed feed rice. *Biosystems Engineering*, 136, 87–91.
- Tolaba, M. P., Peltzer, M., Enriquez, N., & Pollio, M. L. (2004). Grain sorption equilibria of quinoa grains. *Journal of Food Engineering*, 61, 365–371.
- Torrez Irigoyen, R. M., & Giner, S. A. (2011). Volume and density of whole soybean products during hot-air thermal treatment in fluidised bed. *Journal of Food Engineering*, 102, 224–232.
- Torrez Irigoyen, R. M., & Giner, S. A. (2014). Drying-toasting kinetics of presoaked soybean in fluidised bed. Experimental study and mathematical modelling with analytical solutions. *Journal of Food Engineering*, 128, 31–39.
- Torrez Irigoyen, R. M., Goñi, S. M., & Giner, S. A. (2014). Drying-toasting kinetics of presoaked soybean. A mathematical model considering variable diffusivity, shrinkage and coupled heat transfer. *Journal of Food Process Engineering*, 142, 70–79.
- Vazquez, A., & Calvelo, A. (1980). Gas particle heat transfer coefficient in fluidized pea beds. *Journal of Food Process Engineering*, 4, 53–70.
- Vazquez, A., & Calvelo, A. (1983). Gas particle heat transfer coefficient for the fluidization of different shaped foods in fluidized pea beds. *Journal of Food Process Engineering*, 4, 53.